

Appendix

Table 1: Flight path meta-data for the Isangi-Stanleyville aerial survey. Data provided consists of the flight path number, cardinal direction of the flight, the image numbers, and the duration of the flight provided by the start and end time of the acquisition. Data is sourced from Appendix Figure 2 and the sensor logs recorded in the margin of acquired images (see Figure 1 main manuscript).

| path | direction | image # | start (H:M:S) | end (H:M:S) |
|------|-----------|---------------------|---------------|-------------|
| 1 | W – E | 04 / 78 – 04 / 127 | 10:15:00 | 10:40:00 |
| 2 | W – E | 05 / 01 – 05 / 56 | 10:15:00 | 10:40:00 |
| 3 | W – E | 06 / 01 – 06 / 48 | 08:55:00 | 09:20:00 |
| 4 | W – E | 07 / 01 – 07 / 20 | 09:30:00 | 09:45:00 |
| 5 | W – E | 05 / 167 – 05 / 187 | 08:55:00 | 09:10:00 |
| 6 | W – E | 07 / 67 – 07 / 82 | 10:50:00 | 11:00:00 |
| 7 | E – W | 06 / 49 – 06 / 95 | 09:35:00 | 10:05:00 |
| 8 | E – W | 05 / 57 – 05 / 103 | 10:20:00 | 10:50:00 |
| 9 | E – W | 04 / 128 – 04 / 176 | 10:50:00 | 11:10:00 |
| 10 | W – E | 08 / 01 – 08 / 27 | 09:05:00 | 09:20:00 |
| 11 | W – E | 06 / 96 – 06 / 139 | 10:25:00 | 10:45:00 |

Table 2: Site description of all the current permanent sampling plots in the greater Yangambi region. We list the forest type, plot number, geographic location (in decimal degrees), stem density, basal area Above Ground Carbon (AGC), species richness and Land-Use and Land-Cover Change (LULCC) classes in a radius of 100m around each plot location.

| type | nr | latitude | longitude | stem density (ha^{-1}) | basal area ($m^2 ha^{-1}$) | AGC (Mg C ha^{-1}) | species richness | LULCC class coverage (%) |
|----------------|----|-----------|-----------|----------------------------|------------------------------|-----------------------|------------------|--------------------------|
| fallow | 1 | 0.7959139 | 24.49423 | 350 | 5.39000 | 6.7000 | 26 | 37 (1), 63 (3) |
| fallow | 2 | 0.7921028 | 24.49717 | 132 | 2.06000 | 2.0400 | 22 | 68 (1), 32 (3) |
| young-regrowth | 1 | 0.7894028 | 24.51755 | 322 | 20.44000 | 46.5600 | 40 | 68 (1), 32 (3) |
| young-regrowth | 2 | 0.7948806 | 24.49193 | 447 | 16.63000 | 27.8300 | 25 | 56 (1), 44 (3) |
| young-regrowth | 3 | 0.7931083 | 24.49013 | 313 | 17.80000 | 37.1000 | 43 | 51 (1), 49 (3) |
| old-regrowth | 1 | 0.8824444 | 24.49614 | 384 | 19.48000 | 81.7800 | 92 | 100 (1) |
| mixed | 1 | 0.8135486 | 24.51264 | 563 | 34.81000 | 168.0400 | 83 | 100 (1) |
| mixed | 2 | 0.7805000 | 24.52109 | 403 | 35.25000 | 174.5800 | 78 | 100 (1) |
| mixed | 3 | 0.7866181 | 24.52349 | 367 | 30.69000 | 150.3000 | 75 | 100 (1) |
| mixed | 4 | 0.8140333 | 24.49370 | 432 | 33.01000 | 168.6100 | 84 | 100 (1) |
| mixed | 5 | 0.8025611 | 24.48750 | 329 | 25.20000 | 124.1800 | 80 | 100 (1) |
| mixed | 6 | 0.9925556 | 24.53906 | 490 | 32.63000 | 203.8100 | 86 | 100 (1) |
| mixed | 7 | 0.9898056 | 24.53853 | 598 | 31.47000 | 146.1100 | 92 | 100 (1) |
| mixed | 8 | 0.9866111 | 24.53856 | 556 | 29.20000 | 148.2100 | 90 | 100 (1) |
| mono-dominant | 1 | 0.8269306 | 24.52303 | 344 | 31.80000 | 183.0100 | 48 | 100 (1) |
| mono-dominant | 2 | 0.8282708 | 24.53196 | 436 | 32.06000 | 173.5800 | 55 | 100 (1) |
| mono-dominant | 3 | 0.7965903 | 24.49779 | 376 | 30.57000 | 166.4400 | 62 | 100 (1) |
| mono-dominant | 4 | 0.8080889 | 24.52811 | 374 | 27.69000 | 145.5500 | 46 | 100 (1) |
| mono-dominant | 5 | 0.8682806 | 24.45655 | 217 | 27.19000 | 159.0000 | 46 | 95 (1), 5 (2) |
| mono-dominant | 6 | 0.7992278 | 24.49195 | 378 | 33.95000 | 165.4800 | 68 | 100 (1) |
| edge | 1 | 0.7895486 | 24.51990 | 415 | 30.93601 | 152.2792 | 77 | 100 (1) |
| edge | 2 | 0.7979472 | 24.48885 | 368 | 31.82097 | 152.1736 | 72 | 95 (1), 5 (3) |
| edge | 3 | 0.8144250 | 24.48555 | 458 | 35.79959 | 197.4022 | 86 | 100 (1) |
| edge | 4 | 0.7659306 | 24.51125 | 320 | 29.72547 | 154.6380 | 75 | 98 (1), 2 (3) |
| edge | 5 | 0.8691778 | 24.47019 | 459 | 33.72462 | 158.6934 | 88 | 100 (1) |

Table 3: Summary statistics for different forest plot types. We report the mean and standard deviation for Above Ground Carbon (AGC), basal area, stem density values and number of plots (as mentioned in Appendix Table 1).

| forest type | AGC (Mg C ha^{-1}) | stem density (ha^{-1}) | basal area ($m^2 ha^{-1}$) | nr. plots |
|----------------|-----------------------|----------------------------|------------------------------|-----------|
| edge | 163.04 ± 19.39 | 404 ± 60.03 | 32.4 ± 2.39 | 5 |
| fallow | 4.37 ± 3.3 | 241 ± 154.15 | 3.72 ± 2.35 | 2 |
| mixed | 160.48 ± 23.84 | 467.25 ± 99.42 | 31.53 ± 3.26 | 8 |
| mono-dominant | 165.51 ± 12.75 | 354.17 ± 73.56 | 30.54 ± 2.64 | 6 |
| old-regrowth | 81.78 | 384 | 19.48 | 1 |
| young-regrowth | 37.16 ± 9.37 | 360.67 ± 74.9 | 18.29 ± 1.95 | 3 |

ISANGI — STANLEYVILLE (1^{re} Partie)

58/04-05-06-07-08-09-24-25-27-87. 59/07

Date de prises de vues : 6/1/58 au 20/2/58. 26/2/58 au 9/1/59.
Appareil de prises de vues : Camera Wild FCSa - L404 Avigon

Distance focale : 114,83 mm
Altitude objective : 5.200 m
Altitude de survol : 4.600 m.
Altitude approximative au sol : 600 m
Echelle approximative : 1/40.000
Surface couverte : 18.530 Km²

| Bandes | Couverture utile | Genres | Double emploi | à rejeter | Double emploi Couverture plus récente |
|--------------------------|--|------------|---|-----------|--|
| 1 [X 1 X 2 | 58/04/78 à 127 " 05/01 " 56 | Inf. rouge | | | 76 et 77 |
| 2 [X 3 X 4 X 5 | " 06/01 " 48 " 07/01 " 20 " 08/07 " 187 | " | 156 à 166 et 188 à 190 | | 67 " 68 93 " 95 |
| 3 [X 6 X 7 | " 07/69 " 82 " 08/02 " 92 | " | | | 101 " 103 174 " 176 01 " 02 96 " 98 |
| 4 [X 9 X 10 X 11 | " 05/57 " 100 " 04/128 " 173 " 08/03 " 27 | " | | | 46 " 47 64 " 66 181 " 185 177 " 178 48 " 49 270 " 313 01 " 05 98 " 107 314 " 316 |
| 5 [X 12 X 13 X 14 | " 06/199 " 139 " 07/234 " 279 " 08/28 " 45 " 07/21 " 63 | " | 58/07/280 à 323 Couvert par bande 20/12/59 | | |
| 6 [X 15 X 16 | " 06/140 " 180 " 04/179 " 225 | " | | | |
| 7 [X 17 X 18 | " 08/50 " 105 " 06/314 " 318 | " | | | |
| 8 [X 19 X 20 | " 09/06 " 51 " 09/52 " 97 | " | | | |
| 9 [X 21 X 22 | " 04/305 " 313 " 08/106 " 166 | " | | | |
| 10 [X 23 X 24 | " 05/191 " 252 " 25/230 à 299/290-291 | " | | 260 à 279 | 228 " 229 |
| 11 [X 25 X 26 | " 27/128 " 188 " 27/180 " 223 | " | | | 224 " 236 |
| 12 [X 27 X 28 | " 24/209 " 273 " 25/292 " 357 | " | | | |
| 13 [X 29 X 30 X 31 | 59/07/01 " 50 " 97/99 " 101 " 07/74 " 94 | " | 95 à 98 et 102 à 105 | | |
| 14 [X 32 X 33 X 34 | " 07/58 " 68 58/87/01 " 65 " 87/66 " 84 | " | 91 à 97 et 99 à 73 | | |
| 15 [X 35 | 59/07/106 " 148 | " | 85 " 92 | | |

Figure 2: Overview of the complete flight plan meta-data as stored in the archives at the Africa Museum.



Figure 3: Shelves with aerial survey images at the Africa Museum archives, showing vast amounts of historical data still mostly unexplored.

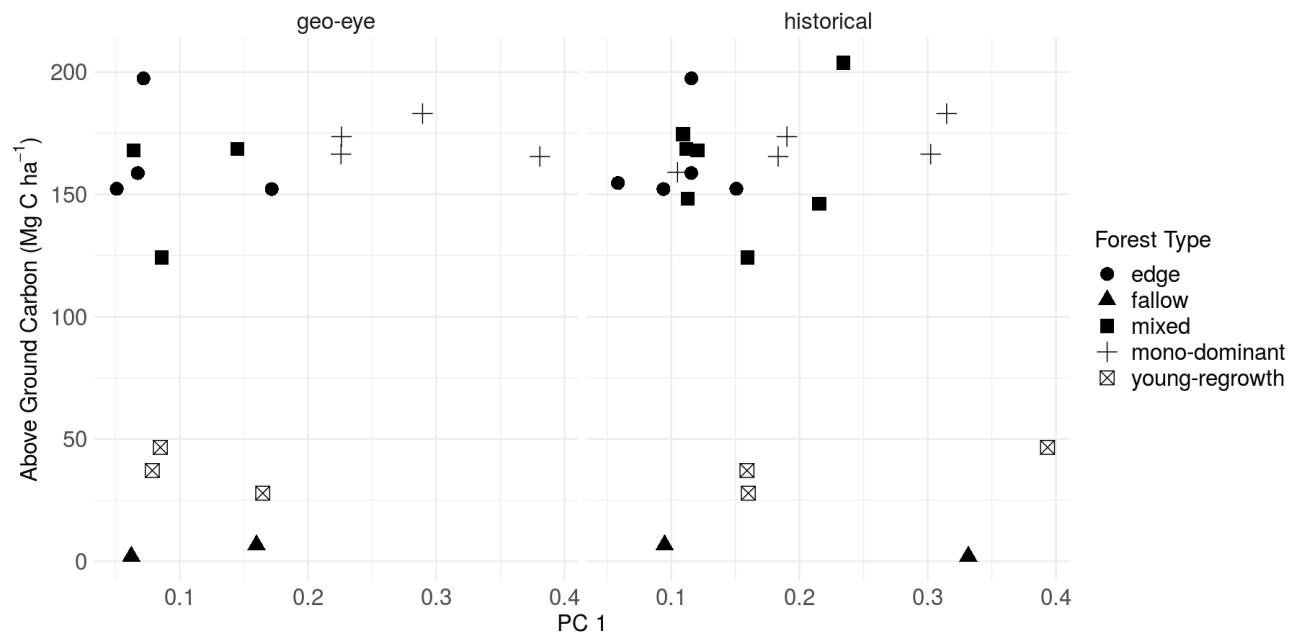


Figure 4: Scatterplot comparing Above Ground Carbon and the first principal component of the FOTO analysis for contemporary Geo-Eye (left) and the historical orthomosaic (right) data. Different forest types are plotted using closed circles, closed triangles, closed squares and this for fallow, mixed mon-dominant and young-regrowth forests, respectively

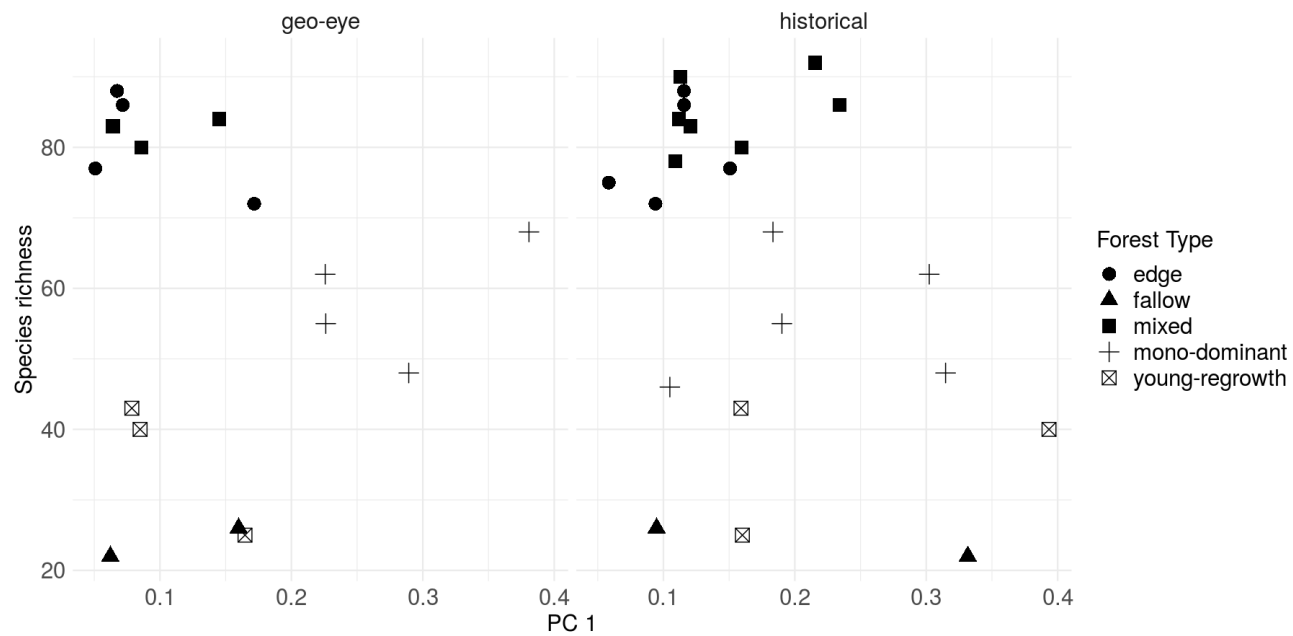


Figure 5: Scatterplot comparing tree species richness and the first principal component of the FOTO analysis for contemporary Geo-Eye (left) and the historical orthomosaic (right) data. Different forest types are plotted using closed circles, closed triangles, closed squares and this for fallow, mixed mono-dominant and young-regrowth forests, respectively

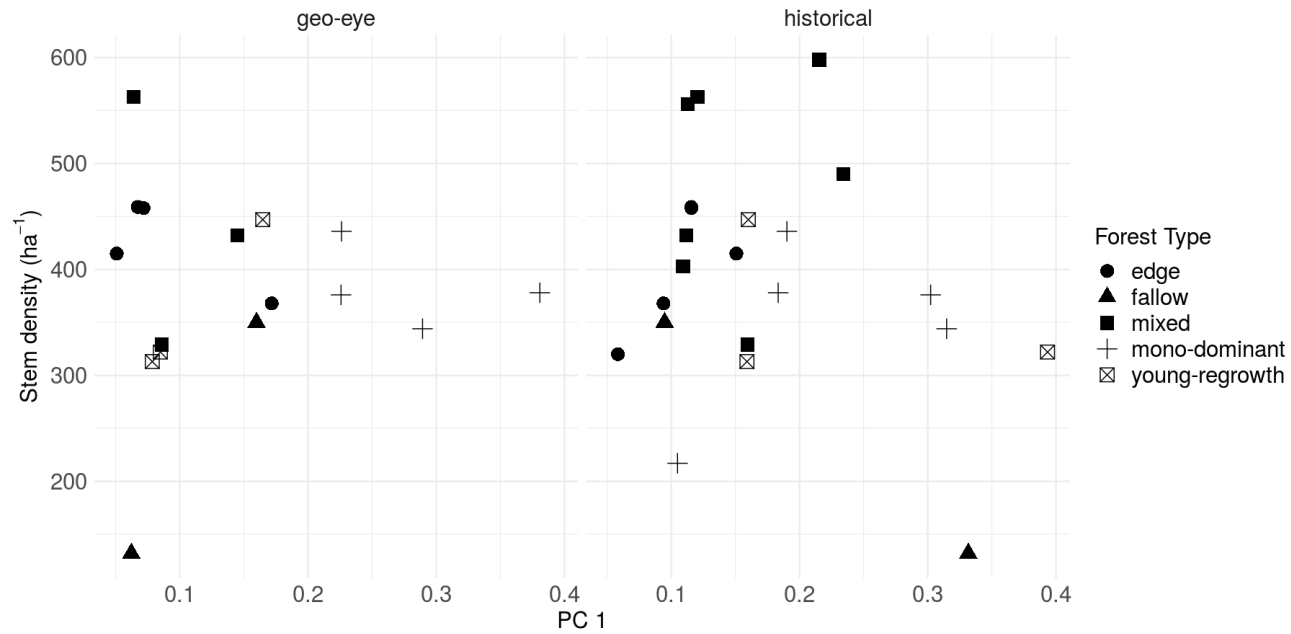


Figure 6: Scatterplot comparing stem density (per ha) and the first principal component of the FOTO analysis for contemporary Geo-Eye (left) and the historical orthomosaic (right) data. Different forest types are plotted using closed circles, closed triangles, closed squares and this for fallow, mixed mono-dominant and young-regrowth forests, respectively